Study of Some Structural, Optical and Electrical Properties of Thin Film Selenium Sulfide Tin Prepared by the Thermal Evaporation Method in Vacuum

Salah El-Din Tariq Mahmoud and Jaafar Sadiq Mohammed
Department of Physics, College of Science, University of Diyala, 32001 Baqubah, Diyala, Iraq
{Sciphyms232404, jafar.mm1967}@uodiyala.edu.iq

Keywords: Vacuum Thermal Deposition, Optical, Structural, Electrical Properties.

Abstract: This research includes the preparation of thin films of $Se_{75}S_{25-x}Sn_x$ by vacuum thermal evaporation method with a thickness of 400 +-20 nm on glass substrates and studying some structural, optical and electrical properties of the film. X-ray examination detect that the film has a random structure at (x=0 and 5) while single crystal growth begins at x=10,15. By measuring the transmittance and absorbance spectra for the wavelength range 400 – 1100 nm it was found that the transmittance decreases and the absorbance increases as a function of wavelength with increasing tin content. The energy gap for the indirect transition allowed was also calculated and shown to decrease with increasing tin content. The Hall effect examination revealed that the film prepared at (x=0 and 5) is of the P type while at x=10, 15 it turns into the N type and that the conductivity increases with increasing tin content and the resistivity decreases.

1 INTRODUCTION

Chalcogenide glasses have gained great importance in recent years due to their advantageous properties, and have been widely used in various solid-state devices. Therefore, the search for new materials for use in device technology is ongoing. Finding new materials that can modify their properties is key to the development of solid-state technology. Semiconductors can be used to manufacture devices with specific properties by controlling the structural, optical, and electrical properties of these materials. Trigonal alloy semiconductors provide such materials [1]. The great interest of researchers is due to the fact that these materials combine the properties of random materials and some of the properties of crystalline semiconductors [2]-[9].Many studies have been conducted on selenium-treated metallic glass with regard to its electrical and optical properties [10]-[20]. Based on this, we use selenium due to its many commercial applications [21], but it has drawbacks in its pure state due to its poor sensitivity and short lifetime. To eliminate these drawbacks, we use some additives, thus obtaining better properties of hardness, sensitivity, conductivity, and lifetime compared to pure selenium [22]. In this system, we used tin in the Se-S system. This addition expands the area of glass formation and causes a disturbance in the composition and structure of the system. [23]

2 MODELING AND WORKING METHODS

Thin films of $Se_{75}S_{25-x}Sn_x$ were prepared using the vacuum evaporation method. The $Se_{75}S_{25-x}Sn_x$ compound was prepared by mixing proportions of each of its constituent elements with a purity of 99.99% and according to the x values of 0, 5, 10, 15%. After determining the mass of the mixture (6g), the mass of each constituent element was calculated using a sensitive electric balance with four-decimal-place accuracy. The mixture was placed in quartz tubes (15cm length). The tubes were evacuated using a mechanical vacuum system to prevent oxidation during heating and sealed with an oxyacetylene torch. They were then placed in an electric furnace and gradually heated from room temperature to 450°C (above the melting points: Se 221°C, S 113°C, Sn 232°C) for two hours. The tubes were angled at 45° to ensure homogeneity and left for 24 hours to cool gradually to room temperature.

After removal from the furnace, the compound was extracted, crushed using a hammer and ceramic bowl, and stored as a powder in clean, dry containers. An appropriate amount of the $Se_{75}S_{25-x}Sn_x$ powder was placed in a molybdenum boat to achieve the required thickness according to the equation *m = 4πptr²* [24]. The evaporation system was prepared by placing the boat between electrodes and fixing thoroughly cleaned substrates on the holder at a distance from the source to dissipate heat and ensure uniform deposition. Film thickness was measured gravimetrically using $t = m/(S \cdot \rho)$ [25].

3 RESULTS AND DISCUSSION

3.1 Structural Properties

3.1.1 X-ray Diffraction

Figure 1 shows the X- ray diffraction patterns of the $Se_{75}S_{25-x}Sn_x$ films. It is evident that at a tin content of 0,5 there are no clear peaks, confirming the random nature of these films. As the tin content increases (10, 15) a single peak begins to appear, becoming more pronounced with increasing tin content. This indicates that increasing the tin content improves the crystallization process [26].

3.1.2 FESEM Analysis

All $Se_{75}S_{25-x}Sn_x$ films were examined using a scanning electron microscope (FESEM) at a magnification of 500 nm to determine the surface texture of the films and observe the effect of tin doping ratios. It was found that varying tin percentages had a clear effect on the surface structure of these films. This is consistent with most studies of the random state in electron microscopy [27]. Figure 2 shows that the films exhibit a random appearance. However, for films doped with 15% tin, we observe the appearance of a granular shape consisting of small, uniform, and almost homogeneous spherical grains.

3.2 Optical Properties

3.2.1 Absorption

The optical properties of $Se_{75}S_{25-x}Sn_x$ films x=0, 5, 10, 15 deposited on glass slides by vacuum evaporation were studied. Figure 3 shows how the absorbance (A) changes as a function of wavelength (λ). We observe that all films have their highest absorbance at wavelengths below 500 nm, reaching (2.75-3.75). This means that the absorbance is highest at the beginning of the visible region, where the energy is greater than the energy gaps for the indirect transitions allowed by the films, which have values of (2 - 1.63ev) and will be presented later. This means that the absorbed photons are able to excite the electrons in the valence band and transfer them to the conduction band. Then we notice a sharp drop in the absorbance at large wavelengths. We also notice that the absorbance increases with the increase in the tin percentage due to the absorption processes formed by the tin doping levels, meaning that the tin levels worked to form local levels between the valence and conduction bands, which worked as auxiliary levels that enabled the electrons that did not absorb enough energy to overcome the energy gap to move from the valence band to the conduction band. Also, the sharp edges were shifted towards the longer wavelengths [28], and the largest shift was at the ratio of 15%.

3.2.2 Transmittance

Transmittance behaves in complete opposition to absorbance.Figure 4 shows the transmittance spectrum as a function of wavelength in the spectrum region (400 - 1100 nm). We note that the transmittance of all prepared films increases with increasing wavelength, up to the near-infrared region, where it reaches 80% at x=0, 70% at x=5, and 30% at x=10.15. This means that transmittance decreases when the material is doped with tin [29]-[30]. The decrease in the transmittance spectrum is attributed to the increased light absorption by the localized levels formed by tin within the prepared energy gap. We also observe the oscillatory behavior of all films, indicating that they are homogeneous.

3.2.3 Optical Energy Gap

The optical energy gap value for the allowed indirect transmission was calculated from the equation $\alpha h\upsilon = \beta(h\upsilon - E_g^{opt})^r$[31] by setting (r = 2). We then draw the relationship between $(\alpha h\upsilon)1/2$ on the y-axis and $(h\upsilon)$ the photon energy on the x-axis see Figure 5. The energy gap is determined from the intersection of the straight line of the curve with the x-axis, represented by the photon energy at $\alpha = 0$. This point represents the energy gap

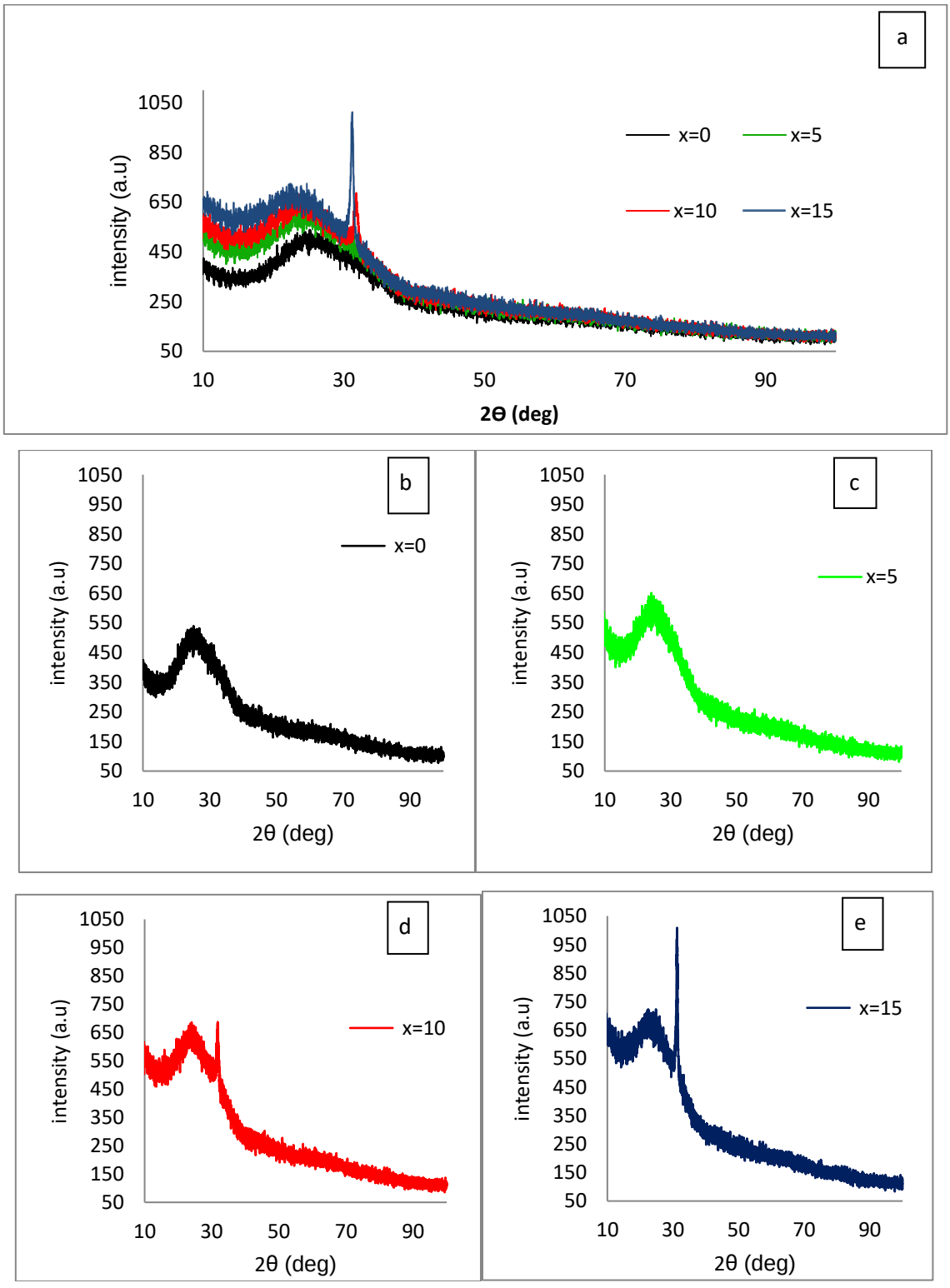

Figure 1: XRD patterns of $Se_{75}S_{25-x}Sn_x$ thin films with different tin concentrations a), b), c), d) and e).

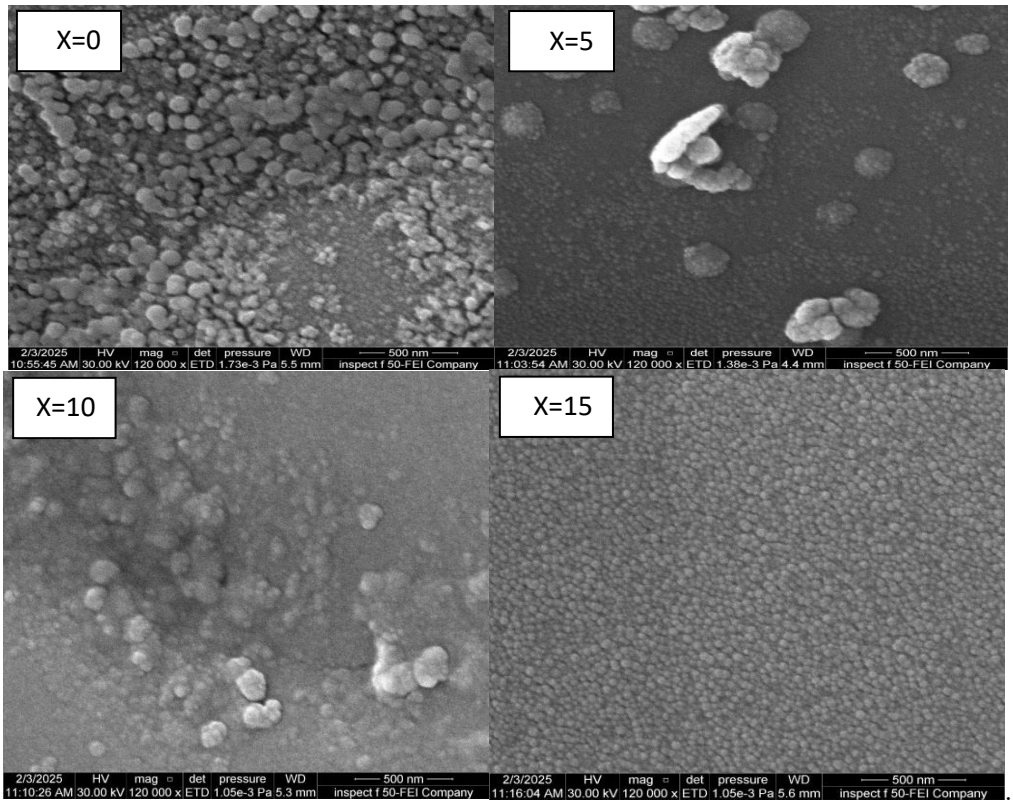

Figure. 2: FESEM micro image of $Se_{75}S_{25-x}Sn_x$ thin film at different concentrations of tin.

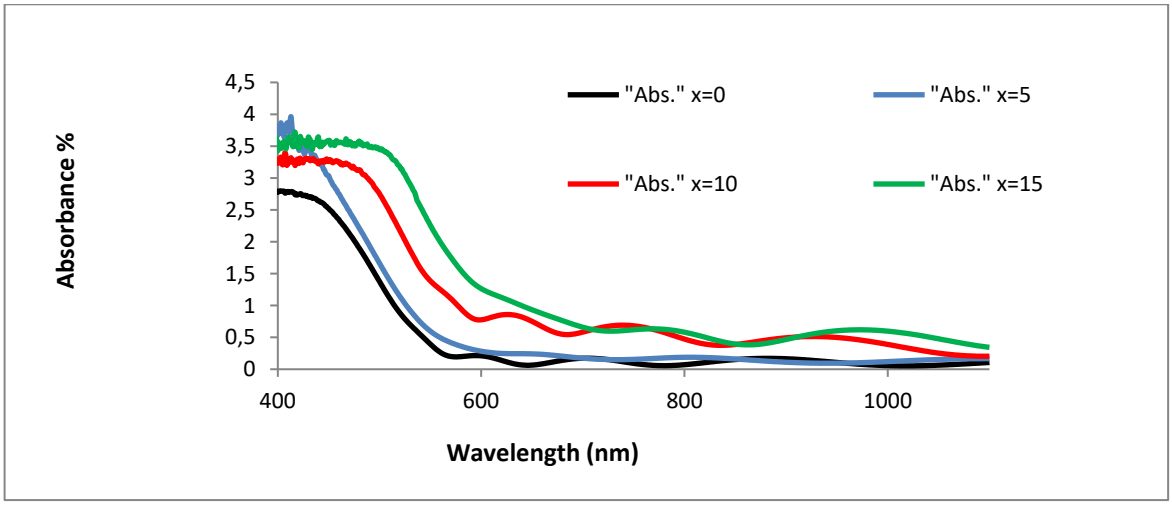

Figure 3: Absorption spectrum as a function of wavelength of $Se_{75}S_{25-x}Sn_x$ thin film at different concentrations of tin.

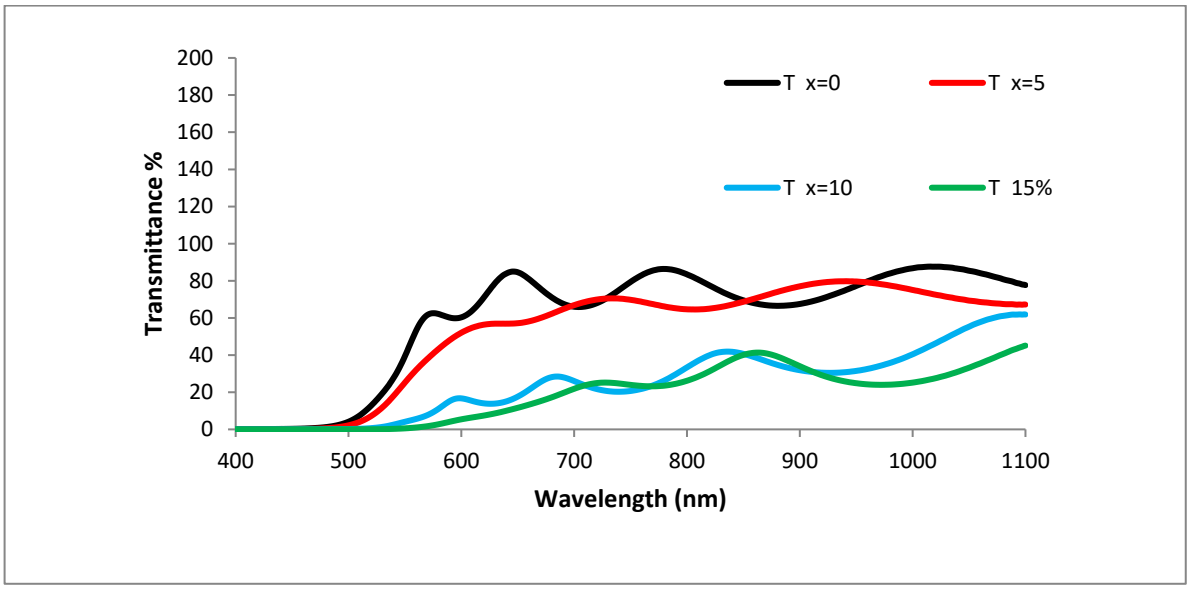

Figure 4: Transmittance spectrum as a function of wavelength of $Se_{75}S_{25-x}Sn_x$ thin film at different concentrations of tin.

Table 1: The energy gap values of $Se_{75}S_{25-x}Sn_x$ thin film at different concentrations of tin.

Concentration x	Eg (ev)
0	2
5	1.9
10	1.73
15	1.63

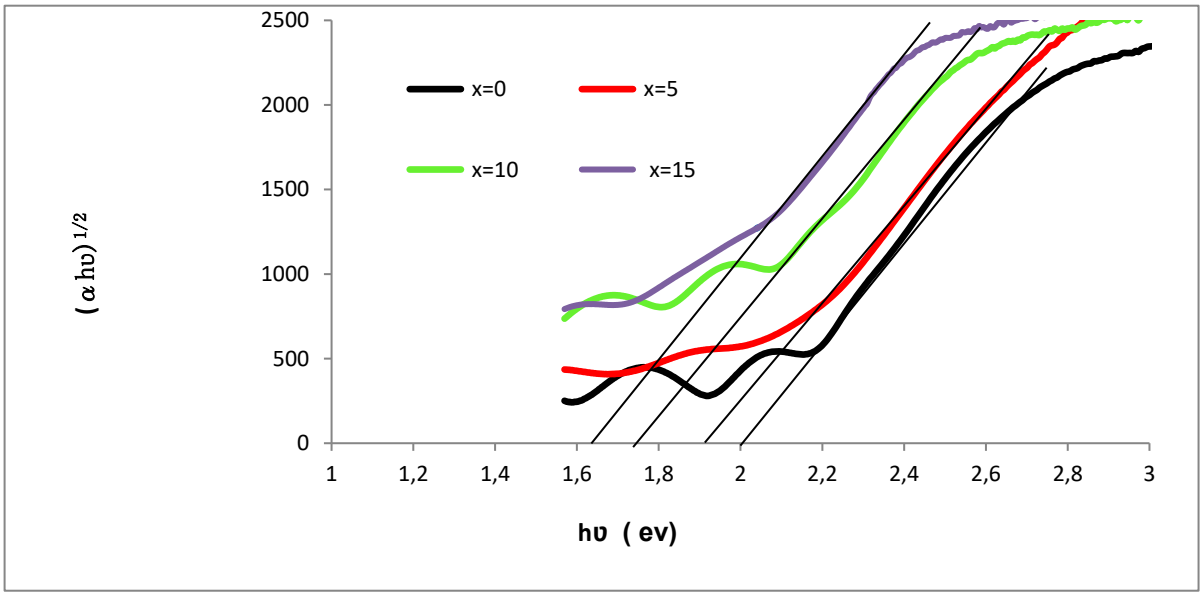

Figure. 5: Change in energy gap for indirect transition allowed for $Se_{75}S_{25-x}Sn_x$ thin film at different concentrations of tin.

Table 2: Hall effect investigation data on $Se_{75}S_{25-x}Sn_x$ thin films.

Concentration	0	5	10	15
RH(cm^3/c) *10^7	1.992	1.610	-0.119	-1.616
N(cm^{-3}) *10^{11}	3.133	3.877	-52.26	-3.433
μ(cm^2/v.s)	41.84	56.36	17.87	580
ρ(Ω.cm) *10^5	4.762	2.857	0.6682	0.3135
σ(Ω.cm)$^{-1}$ *10^{-6}	2.1	3.5	14.97	31.90

value, which changes from 2 eV to 1.63 eV See Table 1, decreasing with increasing doping ratio, i.e., by 0.37 eV. The decrease in the energy gap value with doping with metals is consistent with researcher [32], who used indium, and researcher [33], who used silver. The explanation for this is that tin results in an increase in the density of the localized levels formed by tin atoms within the energy gap

3.3 Electrical

3.3.1 Hall Effect

A room-temperature Hall effect experiment was conducted on $Se_{75}S_{25-x}Sn_x$, x=0.5, 10.15. Thin films are used to determine their electrical properties and to know the concentration, type, and movement of the majority carriers of charge, as well as their conductivity and resistivity. Results in Table 2 show that the conductivity is P- type at x=0.5, where the Hall coefficient is positive, meaning holes are the majority charge carriers while electrons are the minority

However, it transforms to N-type at x=10.15, where the Hall coefficient becomes negative, meaning electrons are the majority carriers, while holes become the minority.

We note that with the increase of tin content, the conductivity increases, reaching its highest value 31.9*10-6 at x=15. The resistivity decreases with increasing tin content

4 CONCLUSIONS

This study demonstrates that tin (Sn) doping significantly modifies the structural, optical, and electrical properties of vacuum-evaporated Se-S thin films. Specifically:

1) X-ray diffraction (XRD) analysis revealed an initially amorphous structure for all films, with crystallinity improving as Sn content increased, evidenced by the emergence of a distinct peak, particularly pronounced at x=15 (confirmed by FE-SEM images).
2) Optical measurements over 400–1100 nm showed decreasing transmittance and increasing absorbance with higher Sn concentrations.
3) The calculated energy gap for the allowed indirect transition decreased with increasing Sn content.
4) Hall effect measurements indicated a transition from p-type to n-type conductivity with increasing Sn. This resulted in significantly increased conductivity and decreased resistivity due to the higher concentration of electron charge carriers provided by the metal dopant.

The practical significance of this work lies in enhancing Se-S properties for potential applications in solar cells, optical filters, and solid-state devices.

REFERENCES

[1] B. A. Ahmed, et al., "The dependence of the energy density states on the substitution of chemical elements in the Se6Te4-xSbx thin film," Chalcogenide Lett., vol. 19, no. 4, pp. 301-308, 2022.

[2] J. S. Mohammed, et al., "Investigating the optical and electrical characteristics of As60Cu40-xSex thin films prepared using pulsed laser deposition method," Chalcogenide Lett., vol. 20, no. 7, 2023.

[3] S. H. Salman, S. M. Ali, and G. S. Ahmed, "Study the effect of annealing on structural and optical properties of indium selenide (InSe) thin films prepared by vacuum thermal evaporation technique," J. Phys.: Conf. Ser., vol. 1879, no. 3, 2021.

[4] N. Mehta, K. Singh, and A. Kumar, "On the glass transition phenomenon in Se–Te and Se–Ge based ternary chalcogenide glasses," Physica B, vol. 404, no. 12-13, pp. 1835-1839, 2009.

[5] J. Rocca, et al., "Crystallization process on amorphous GeTeSb samples near to eutectic point Ge15Te85," J. Non-Cryst. Solids, vol. 355, no. 37-42, pp. 2068-2073, 2009.

[6] Z. Khan, S. Khan, and M. Alvi, "Study of glass transition and crystallization behavior in Ga15Se85-xPbx ($0 \leq x \leq 6$) chalcogenide glasses," Acta Phys. Pol. A, vol. 123, no. 1, pp. 80-86, 2013.

[7] B. Venugopal, et al., "Influence of manganese ions in the band gap of tin oxide nanoparticles: structure, microstructure and optical studies," RSC Adv., vol. 4, no. 12, pp. 6141-6150, 2014.

[8] I. Madwar, "A theoretical approach to studying indium addition on some physical properties of chalcogenides," Damascus Univ. J. Basic Sci., vol. 36, no. 1, 2020.

[9] A. M. Abd Elnaeim, et al., "Glass transition and crystallization kinetics of Inx(Se0.75Te0.25)100−x chalcogenide glasses," J. Alloys Compd., vol. 491, no. 1-2, pp. 85-91, 2010.

[10] A. Abu El-Fadl, et al., "Calorimetric studies of the crystallization process in Cu10Se90 and Cu20Se80 chalcogenide glasses," Physica B, vol. 398, no. 1, pp. 118-125, 2007.

[11] N. Suri, et al., "Calorimetric studies of Se80−xTe20Bix bulk samples," J. Non-Cryst. Solids, vol. 353, no. 13-15, pp. 1264-1267, 2007.

[12] A. A. Othman, K. A. Aly, and A. M. Abousehly, "Crystallization kinetics in new Sb14As29Se52Te5 amorphous glass," Solid State Commun., vol. 138, no. 4, pp. 184-189, 2006.

[13] M. A. Abdel-Rahim, M. M. Hafiz, and A. M. Shamekh, "A study of crystallization kinetics of some Ge–Se–In glasses," Physica B, vol. 369, no. 1-4, pp. 143-154, 2005.

[14] V. S. Shiryaev, et al., "Study of characteristic temperatures and nonisothermal crystallization kinetics in AsSeTe glass system," Solid State Sci., vol. 7, no. 2, pp. 209-215, 2005.

[15] Z. G. Ivanova and E. Cernoskova, "Study on glass transition and crystallization kinetics of GexSb40−xSe60 glasses by differential thermal analysis," Thermochim. Acta, vol. 411, no. 2, pp. 177-180, 2004.

[16] K. S. Bindra, et al., "Structural and transport properties of amorphous Se–Sb–Ag chalcogenide alloys and thin films," Thin Solid Films, vol. 516, no. 2-4, pp. 179-182, 2007.

[17] G. Dong, et al., "Study of thermal and optical properties of GeS2–Ga2S3–Ag2S chalcogenide glasses," Mater. Res. Bull., vol. 42, no. 10, pp. 1804-1810, 2007.

[18] A. Abu El-Fadl, et al., "Annealing effects on the optical parameters of Cu10Se90 and Cu20Se80 films deposited by evaporation technique," Physica B, vol. 382, no. 1-2, pp. 110-117, 2006.

[19] A. Thakur, et al., "Optical properties of amorphous Ge20Se80 and Ag6(Ge0.20Se0.80)94 thin films," Opt. Mater., vol. 30, no. 4, pp. 565-570, 2007.

[20] P. Sharma and S. C. Katyal, "Optical study of Ge10Se90−xTex glassy semiconductors," Thin Solid Films, vol. 515, no. 20-21, pp. 7966-7970, 2007.

[21] S. A. Khan, et al., "Effect of cadmium addition on the optical constants of thermally evaporated amorphous Se–S–Cd thin films," Curr. Appl. Phys., vol. 10, no. 1, pp. 145-152, 2010.

[22] S. K. Srivastava, P. K. Dwivedi, and A. Kumar, "Steady state and transient photoconductivity in amorphous thin films of Se100-xInx," Physica B, vol. 183, no. 4, pp. 409-414, 1993.

[23] S. A. Khan, et al., "Kinetics of Se75S25−xCdx glassy system using differential scanning calorimeter," J. Alloys Compd., vol. 484, no. 1-2, pp. 649-653, 2009.

[24] S. M. Sze, Semiconductor Devices: Physics and Technology, John Wiley & Sons, 2008.

[25] A. Abu El-Fadl, E. M. El-Maghraby, and G. A. Mohamad, "Influence of gamma radiation on the absorption spectra and optical energy gap of Li-doped ZnO thin films," Cryst. Res. Technol., vol. 39, no. 2, pp. 143-150, 2004.

[26] A. A. Al-Ghamdi, M. A. Alvi, and S. A. Khan, "Non-isothermal crystallization kinetic study on Ga15Se85−xAgx chalcogenide glasses by using differential scanning calorimetry," J. Alloys Compd., vol. 509, no. 5, pp. 2087-2093, 2011.

[27] A. Aparimita, et al., "Photo- and thermally induced property change in Ag diffusion into Ag/As2Se3 thin films," Appl. Phys. A, vol. 124, 2018, pp. 1-10.

[28] J. I. Pankove, Optical Processes in Semiconductors, Courier Corporation, 1975.

[29] R. Chauhan, et al., "Linear and nonlinear optical changes in amorphous As2Se3 thin film upon UV exposure," Prog. Nat. Sci.: Mater. Int., vol. 21, no. 3, pp. 205-210, 2011.

[30] V. Ilcheva, et al., "Optical properties of thermally evaporated (As2Se3)100-xAgx thin films," Phys. Procedia, vol. 44, pp. 67-74, 2013.

[31] M. S. Dresselhaus and M. S. Dresselhaus, Optical Properties of Solids, Part II, 1998.

[32] G. A. M. Amin, "Studies on Inx(As2Se3) thin films using variable angle spectroscopic ellipsometry (VASE)," Mater. Sci. Poland, vol. 33, no. 3, pp. 501-507, 2015.

[33] A. Aparimita, et al., "Photo- and thermally induced property change in Ag diffusion into Ag/As2Se3 thin films," Appl. Phys. A, vol. 124, 2018, pp. 1-10.